において、細胞を移植しなかった群に比べて、さらに、移植後２週目において、心臓幹細胞シート単独移植群と比べて、有意な心機能改善効果（LVFS、左室内径短縮率）が検出された（図６）。血管内皮前駆細胞は、虚血領域において血管新生能力があるという事を考慮すると、同時に移植された血管内皮前駆細胞が血管新生を促進して、虚血領域である梗塞部位に移植された心臓幹細胞シートの生着を助けたと考えられた。この点に関しては、今後、心臓幹細胞シート単独移植群と心臓幹細胞シートと血管内皮前駆細胞の同時移植群において、移植後４週目等の時点で生着細胞数を定量する事に依り、検証可能だと考えられた。

(iii)細胞移植後４週目における組織学的評価

細胞移植後４週目における組織学的な解析の結果、組織の線維化（左室全体に対してや非梗塞領域における線維化率）や心筋細胞の肥大化の程度に関しては、全ての群で有意な差は検出されなかった。我々が用いた実験動物モデルでは、心筋梗塞作製後２週間後に細胞を移植している為、心臓内における線維化や心筋細胞の肥大化は既に完成しており、細胞の移植に依ってもそれらの症状が改善する事がなかったと考えられた。梗塞境界領域における vWF 陽性血管数に関しても、各群間で有意な差が検出されなかった。vWF は、成熟した血管に存在する血管内皮細胞から発現されると考えられているので、移植した血管内皮前駆細胞は、少なくとも移植後４週目の時点において、成熟した血管の形成を促進したとは考えられなかった。しかし、移植後４週目の時点で血管内皮前駆細胞の移植に依り誘導された血管が成熟するかどうかは不明である為、今後は、血管内皮前駆細胞を同時に移植した群において、より早期に形成される毛細血管の数を評価し、その血管新生効果に関して改めて解析する予定である。最後に、心臓幹細胞シートと血管内皮前駆細胞を同時に移植した群において、移植後４週目の時点において移植した細胞が残存しているか確認した所、移植したヒト細胞(HLA 陽性細胞)が残存していた（図７）。さらに、これらの細胞の幾つかは、心筋細胞のマーカーである Cardiac troponin I、血管平滑筋マーカーである alpha Smooth muscle actin、また、血管内皮細胞のマーカーである vWF を発現していた。これらの結果から、心臓幹細胞シートと血管内皮前駆細胞を同時に移植した群においては、移植した細胞のどちらか、或いは両方（心臓幹細胞と血管内皮前駆細胞）がそれらの細胞へ分化し、これらの群で確認された有意な心機能改善効果に寄与したと考えられた。今後は、これら心臓幹細胞シート（女性由来）と血管内皮前駆細胞（男性由来）の同時移植群において、Y 染色体に対する FISH(Fluorescence In Situ Hybridization)等を行い、その群における治療機序を解明する必要があると考えられた。

（３）ブタ慢性心筋梗塞モデルを用いたヒト心臓幹細胞（hCSC）シート移植およびヒト血管内皮前駆細胞（hEPC）心筋内投与併用療法の前臨床試験

Ａ．研究目的

これまでの小動物実験により、積層化した hCSC シートと hEPC 心筋内併用療法の治療効果が確認された。本検討では将来的な臨床試験を目指し、ブタ大動物モデルを用いて、hCSC シートと hEPC 心筋内投与併用療法の安全性および治療効果を検討することを目的とした。

Ｂ．研究方法

移植に用いた心臓幹細胞、心臓幹細胞シートの調製は、上述（(２）の項）と同様に行った。ただし、用いた心臓幹細胞の継代数は、実際の臨床試験を想定し、P5 の細胞を用いた。ミニブタの左前下行枝にアメロイドリングを装着し、梗塞モデルを作成。梗塞作成４週間後に、hCSC シート移植＋hEPC 心筋内投与群(n=1)、hCSC シート単独移植群(n=1)、Sham 群(n=5)

の3群に群別、全身麻酔・気管内挿管の後、左開胸下で細胞移植治療を行った。hCSC シート(3.3×10^7 cells/シート/100mm UpCell)は梗塞部位に積層（3枚/pig）移植、hEPC(2.5×10^6 cells/pig)は境界部位計12カ所(200 ul/site x12/pig)への心筋内投与とした。移植直後にホルター心電図検査、移植8週後に心臓超音波検査を実施し、治療効果を判定した。

C．研究結果

術後全例で耐術し、8 週間の経過観察ができた。移植直後のホルター心電図検査上、いずれの群においても致死性不整脈は認めなかった。移植前の心臓超音波検査でのEF(%)はhCSCシート移植＋hEPC投与群39.6%、hCSC シート単独移植群 37%、Sham 群 32.1±5.2%と画一的に慢性梗塞モデルが作成できた。移植 8 週後の心臓超音波検査上、移植前に比し Sham群ではEF(%)の改善は認めず(1.8%)。一方、hCSC シート群では7.9%のEFの改善を認め、hCSC シート＋hEPC 併用群では11.3%と治療効果の増大が確認された。

D．考察

本検討では将来的なヒト臨床試験と同様のアプローチでの細胞移植に成功し、その手法を確立した。また全例が耐術し、経過観察期間中、致死性不整脈を含めた主要な有害事象を認めず、これらの細胞移植の安全性を確認した。さらにこれまでの小動物実験同様、慢性心筋梗塞モデルに対する hCSC シートとhEPC 併用による左室収縮能の改善効果が確認された。今後は心臓カテーテルや心臓ＣＴでのより詳細な心臓生理学的評価に加え、心筋マッピングでの電気生理学的評価を実施する予定であり、これらの包括的評価の後、臨床応用の際のプロトコールを作成する予定である。

E．健康危険情報　特記なし

F．研究発表

1）　論文発表　特記なし

2）　学会発表

1. 松田剛典、宮川繁、秋丸裕司、堀井美希、齋藤充弘、川本篤彦、浅原孝之、澤　芳樹、心筋再生治療の為のヒト心臓由来C-Kit陽性細胞に対する維持培養法の検討、第１０回再生医療学会、２０１１年３月１日、京王プラザホテル、東京、日本

2. Takenori MATSUDA, Daisuke YOSHIOKA, Shigeru MIYAGAWA, Miki KOMATSU, Hiroshi AKIMARU, Atsuhiro SAITO, Atsuhiko KAWAMOTO, Takayuki ASAHARA, Yoshiki SAWA, 75th Japanese Circulation Society, ２０１１年３月２０日、パシフィコ横浜、横浜、日本（但し、震災の為、中止）

G．知的財産権の出願・登録状況

1. 特許取得　特記なし
2. 実用新案登録　特記なし
3. その他　特記なし

厚生労働科学研究費補助金（再生医療実用化研究事業）

分担研究報告書

増殖因子分泌におけるヒト心筋幹細胞の優位性評価

分担研究者　清水達也　東京女子医科大学先端生命科学研究所　教授

研究要旨；近年心臓に対する細胞移植は、パラクライン効果により心機能を改善すると考えられており、その観点での移植細胞ソースの差別化は重要である。今回ヒト心筋幹細胞の分泌蛋白発現を、ヒト間葉系細胞、ヒト骨格筋芽細胞と比較検討したところ、VEGF、bFGF の発現は有意に高く、また単一細胞状態よりもシート化することにより発現が亢進することが明らかとなった。またこの発現は notch シグナルの活性化により制御されていることも明らかとなった。以上よりヒト心筋幹細胞シート移植は、効果的な細胞ソースと考えられる。

A．研究目的

重症心不全を対象とした幹細胞移植は、全世界で精力的に研究されている。近年多くの細胞移植における心臓機能改善の機序として、移植細胞の分泌する増殖因子とホスト心臓との相互作用によるパラクライン効果が注目されている。多くの細胞が移植細胞ソースとして検討される中で、増殖因子分泌能を指標にした細胞の差別化は、効果的細胞種の選別および機能評価の点で非常に重要と考えられる。

従来心臓への細胞移植は、経冠動脈および直接心筋への注入移植など、細胞浮遊液が使用されてきた。これまでの我々の検討により、細胞をシート化して移植することにより、移植後の生着が改善し、より効果的に心臓機能を改善させることが確認されている。一方で、シート化による分泌蛋白発現への影響については不明である。

今回ヒト心筋幹細胞の分泌蛋白発現を検討し、かつシート化による発現変化、さらにその機序を明らかにすることを目的とする。

B．研究方法

1)細胞間の分泌蛋白の比較検討

移植細胞ソース間での分泌蛋白発現を比較検討するため、ヒト心筋幹細胞(c-kit 陽性細胞)、ヒト骨格筋芽細胞、ヒト骨髄間葉系細胞の培養上清を回収し、ELISA により、VEGF、bFGF の発現を検討する。

2)シート化による分泌蛋白発現への影響

上記各細胞を、次の 3 群で比較する。1)非コンフルエント、2)コンフルエント、3)細胞シート。まず各条件に適した各細胞播種密度を検証する。播種後 24 時間目に、シート群は一度 20℃の培養槽に移して、シートを回収し、皿上にシートのまま新たな培地(血管内皮細胞用培地(増殖因子無)とともに再播種する。他の群に関しては、播種 24 時間目に上記培地へ交換を行う。培養上清は細胞播種48時間目に回収する。なお、各細胞種および各培養条件では、培養皿中の細胞数が異なるため、分泌蛋白量の解析にあたっては、上清回収時の細胞数を計測し、細胞 1 個当たりの蛋白量として評価する。

3)培養上清を用いた血管内皮細胞の管腔構造評価

HUVEC を matrigel 上で培養し、各培養上清添加による管腔形成能を評価する。

4)心筋幹細胞シートの VEGF 発現における notch シグナルの検証

上記 2)の条件における心筋幹細胞の notch シグナルの発現を western blot で評価する。またシート再播種後に、γ secretase inhibitor を添加し、24 時間後に培養上清を回収し、VEGF の発現を評価するとともに、血管内皮細胞の管腔形成能を評価する。

C．研究結果

ヒト心筋幹細胞の培養上清中の VEGF、bFGF 濃度は、ヒト骨格筋芽細胞、ヒト間葉系細胞培養上清に比して有意に高かった。またこの差は、コンフルエント、細胞シート状態でより顕著であった。また培養上清を matrigel 上で培養した HUVEC に添加したところ、増殖因子の濃度の同様に、ヒト心筋幹細胞培養上清を添加した群で管腔形成能が亢進し、さらにコンフルエント培養、細胞シートから回収した培養上清ではより管腔形成能が亢進した。以上よりヒト心筋幹細胞は、ヒト骨格筋芽細胞、ヒト骨髄間葉系細胞より、多くの血管新生増殖因子を産生し、またこの産生された増殖因子は血管新生作用として機能的であると考えられる。

次に、ヒト心筋幹細胞シートにおける VEGF の発現と Notch シグナルとの関連を検討した。非コンフルエント群、コンフルエント群、さらに細胞シート群より細胞抽出液を回収し、western blot により Notch シグナルの活性化を評価した。するとコンフルエント群、シート群において Cleaved Notch-1 の発現が非コンフルエント群に比して亢進していることが確認されたことから、ヒト心筋幹細胞では、シートが形成されるようなコンフルエントな環境では notch シグナルが活性化されていると考えられた。

最後に活性化された Notch シグナルとヒト心筋幹細胞における VEGF 産生との関連を明らかにするために、細胞シート形成後に、γ secretase inhibitor を添加し、24 時間後に培養上清を回収した。すると培養上清中の VEGF は、コントロールに比して有意に低下しており、またこの培養上清添加では、HUVEC の管腔形成が抑制されることが明らかとなった。以上より、ヒト心筋幹細胞シートにおける顕著な血管新生促進効果の機序として、Notch シグナルの活性化に伴う VEGF の産生亢進が関与していると考えられた。

D．考察

細胞移植のソースとして種々の幹細胞が使用される一方で、その差異は必ずしも明らかでない。今回ヒト心筋幹細胞は、従来使用されている筋芽細胞や骨髄間葉系細胞よりも多くの血管新生増殖因子を産生しており、また機能的にも血管新生を促進することが明らかとなった。さらに従来単一細胞を心筋内に直接注入するなどの移植方法が一般的に使用されているが、その効果は限定的である。今回いずれの細胞においても、シートを形成しうるコンフルエントな状況で培養することにより、より多くの血管新生増殖因子が産生されることも明らかとなったことから、細胞移植方法としての細胞シート移植の有用性が明らかとなったと考えられる。

腫瘍など血管新生が盛んな組織では notch シグナルの活性化が認められ、また腫瘍細胞では notch シグナル依存性に VEGF の産生が報告されている。細胞シートは単層の組織片と考えられ、積層化しより厚い組織を構築するにおいては、より多くの血管が必要であることからも、細胞シートにおける notch シグナルと血管新生との関連は、血管床の少なさからくる積層化の限界を解決する一助となると考えられる。

E．結論

ヒト心筋幹細胞は、他の組織幹細胞に比して血管新生促進効果が強く、またこの効果はシート化することによって、より大きくなった。心筋幹細胞シート移植は、細胞ソースおよび移植法の観点から非常に有効性の高い治療法につながると考えられる。

F．健康危険情報　特記なし

G．研究発表

1. 論文発表 特記なし

2. 学会発表

松浦勝久 The novel regulatory mechanisms of cellular function in cell therapy for heart failure 第14回日本心不全学会学術集会 2010年10月8日 Journal of Cardiac Failure Vol.16, 2010

松浦勝久 Vascular network formation in cell sheet transplantation and bioengineered three-dimensional tissues 第18回日本血管生物医学会 2010年12月3日 抄録集(2010年)

Basic Cardiovascular Science 2010 Scientific Sessions, 2010.7.22, Palm Springs, T. Shimizu, "Myocardial Tissue Engineering with Cell Sheets."

XXth World Congress of the International Society for Heart Reserch, 2010.5-13-16, Kyoto, T. Shimizu, "Cell sheet approach for cardiac repair."

H．知的財産権の出願・登録状況

1. 特許取得 特記なし

2. 実用新案登録 特記なし

3.その他 特記なし

I．研究協力者

松浦勝久 東京女子医科大学 先端生命医科学研究所

厚生労働科学研究費補助金（再生医療実用化研究事業）

分担研究報告書

心・血管系細胞ハイブリッドシート作成を目的とした心筋幹細胞由来血管内皮細胞の分化法の確立

分担研究者　増田治史　東海大学医学部　基盤診療学系　再生医療科学　准教授

CSC シートのより多層化を実現するために、CSC 誘導心筋シートと CSC 由来血管内皮シートのハイブリッドシートの開発を目的として、流れずり応力と低酸素による CSC の血管内皮細胞への分化誘導を試みた。いずれも血管内皮細胞への分化誘導が可能であった。このことは、同一の CSC から代表研究者が開発した手法により心筋細胞を誘導するとともに、液性因子や成長因子以外の流れずり応力と低酸素を用いて血管内皮細胞に誘導することが可能であり倫理的にも許容できるものである。すなわち、流れずり応力と低酸素を用いて重層化した CSC シートを開発できることが示された。

A．研究目的

CSC を虚血心筋に移植する場合に、CSC を培養してシート状の細胞群を幾層に重ねる必要がある。その際に心筋のみでは栄養や酸素の不足により 5 層以上重ねることができない。したがってより重層にするためには血管を構築することが大切になってくる。今回我々は、CSC シートのより多層化を実現するために、血管構築を同時に惹起させるために流れずり応力と低酸素による CSC 由来血管内皮細胞の誘導を試みた。

B．研究の方法

1）CSC の培養

心筋細胞をボランティアから採取し、c-Kit 陽性細胞を磁気ビーズを用いて精製した。この細胞を 10cm-dish (BD FALCON, 35-3003) で 10% Fetal Bovine Serum (Hyclone, SH30406.02)、5mU/ml ヒトエリスロポエチン(Sigma, E5627-10UN)、10ng/ml bFGF(PEPROTECH, 100-18B)、0.2mM L-Glutathion (GSH) (Sigma, G6013)、Penicillin/Streptomycin を添加した Ham's F12 medium (Wako, 087-08335) で培養し 6～7 回継代した。内皮分化用の培地として 20% FBS (JRH Bioscience 3G0266)と Penicillin/Streptomycin を加えた human Endothelial SFM basal growth medium (GIBCO 11111-044)で 1 日培養した。

2）流れずり応力負荷実験

回転円盤型流れ負荷装置を用いて層流流れずり応力を細胞に負荷した。CSC を含んだ培養皿を装置の台座に置き、ステンレス製の円盤を培養皿の底に置いた。円盤を回転させると培養液に同心円状の流れが生じ、それによって細胞に層流流れずり応力が負荷される。流れずり応力の強さ（τ）は、$\tau = \mu \cdot r \omega / d$ で計算される。ここで、μ は粘度を、r は培養皿の中心からの距離を、ω は回転角速度を、d は回転円盤と培養皿との距離を表す。その装置は、培養皿の中心からの距離に依存した流れずり応力の勾配を生じる。培養皿の細胞は全て使われ、この実験で使用した流れずり応力は 0.1～2.5 dyn/cm^2 であった。全ての実験は CO_2 インキュベーター内 37℃で行なった。

3）低酸素実験

パーソナルマルチガスインキュベーター（ASTEC、APM-30DR）内に細胞を入れて 5%O2、5%CO2 で培養し

た。

4）フローサイトメトリーによる解析

細胞表面蛋白の発現率を KDR-PE (R&D)、VE-cadherin-PE (Beckman Coulter)、PECAM-PE(BD Bioscience)、Tie2-APC (R&D)で染色し、FACS Caliber (Becton Dickinson)で測定した。

5）増殖能

50ng/ml VEGFあるいは20ng/ml SCF負荷による培養1日後ミトコンドリア脱水素酵素によるテトラゾリウム塩 (WST8) のホルマザン色素への変換をELISAで定量した。

6）抗アポトーシス能

100ng/ml TNFaを負荷して1日培養後アポトーシスしたDNA断片をELISAで定量した。

7）脈管形成能

Biocoat Matrigel (Becton Dickinson)で培養して観察し、完全な円の数を定量した。

8）統計学的解析

ANOVA により検定を行い、$P<0.05$ を有意差とした。全ての計算は SPSS ソフトウェアを用いて行った。

C．研究結果

1）形態学的変化

静的条件下および低酸素条件下では細胞の配列は一定の方向性を示さなかった。一方流れずり応力条件下では流れの方向に細胞が伸展・配勾した。この反応は血管内皮細胞に特異的であり、CSC が流れずり応力により血管内皮細胞に分化誘導されたことを示す。

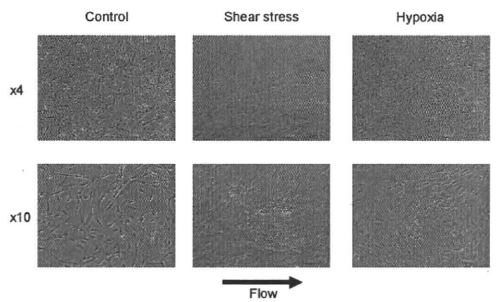

Fig.1. Effect of shear stress and hypoxia on morphology.

2）蛋白発現変化

血管内皮のマーカーである KDR と Tie2 は、流れずり応力負荷および低酸素負荷いずれも発現率が増大した。一方 Flt1、VE-cadherin、PECAM は変化を認めなかった。

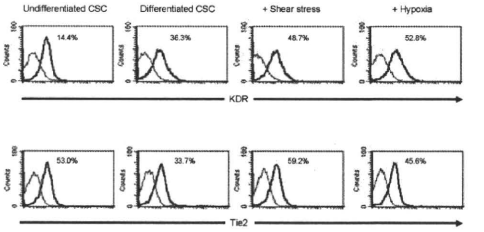

Fig.2. Effect of shear stress and hypoxia on protein expression.

3）増殖能

流れずり応力負荷と低酸素負荷いずれも増殖能が増大した。

4）抗アポトーシス能

流れずり応力条件下と低酸素条件下いずれも TNFα負荷によるアポトーシスは減少していた。このことは流れずり応力と低酸素により抗アポトーシス能が増大したことを意味する。

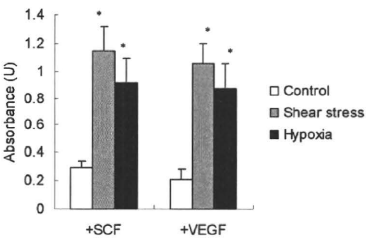

Fig.3. Effect of shear stress and hypoxia on proliferation.
* $P<0.01$ vs. static control.

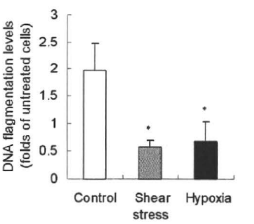

Fig.4. Effect of shear stress and hypoxia on apoptosis.
* $P<0.05$ vs. static control.

5）脈管形成能

流れずり応力負荷と低酸素負荷いずれも脈管形成能は増大した。

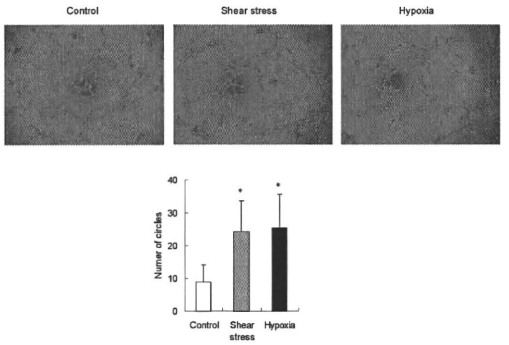

Fig.5. Effect of shear stress and hypoxia on tube formation.
* $P < 0.05$ vs. static control.

D．考察

流れずり応力と低酸素いずれもCSCを血管内皮に分化誘導した。このことは、同一のCSCを代表研究者が開発した手法により心筋細胞を誘導するとともに、今回の手法により流れずり応力と低酸素を用いて血管内皮細胞に誘導し、ハイブリッドシートを作成しより重層化したCSCシートを開発できることが期待できる。

F．健康危険情報　特記なし。

G．研究発表

1）学会発表

第8回 ISSCR Annual Meeting、Development of in vitro single cell based culture system to assess stem cell fate into endothelial lineage. 2010.6.16-19

第10回日本再生医療学会、Single cellによる造血幹細胞からの内皮系細胞系列決定、分化における細胞内情報伝達機構の解析. 2011.3.1-3.2

2）論文発表

「心血管再生の基礎研究」, 心臓（日本心臓財団)、42巻12号、2010年12月

H．知的財産権の出願・登録状況

（予定を含む。）

1. 特許取得　特記なし。
2. 実用新案登録　特記なし。
3. その他　特記なし

Ⅲ　研究成果の刊行に関する一覧表

原著論文

発表者氏名	論文タイトル	発表誌名	巻号	ページ	出版年
Matsumoto T, Ii M, Nishimura H, Shoji T, Mifune Y, Kawamoto A, Kuroda R, Fukui T, Kawakami Y, Kuroda T, Kwon SM, Iwasaki H, Horii M, Yokoyama A, Oyamada A, Lee SY, Hayashi S, Kurosaka M, Takaki S, Asahara T.	Lnk-dependent axis of SCF-cKit signal for osteogenesis in bone fracture healing.	J Exp Med	27;207(10)	2207-23	2010
Kuroda R, Matsumoto T, Miwa M, Kawamoto A, Mifune Y, Fukui T, Kawakami Y, Niikura T, Lee SY, Oe K, Shoji T, Kuroda T, Horii M, Yokoyama A, Ono T, Koibuchi Y, Kawamata S, Fukushima M, Kurosaka M, Asahara T,	Local Transplantation of G-CSF-Mobilized CD34+ Cells in a Patient with Tibial Nonunion: A Case Report.	Cell Transplant	Epub ahead of print	Epub ahead of print	2010
Alev C, Ii M, Asahara T.	Endothelial Progenitor Cells: A "Novel" Tool for the Therapy of Ischemic Diseases.	Antioxid Redox Signal	Epub ahead of print	Epub ahead of print	2011

学会発表 抄録

発表者氏名	発表タイトル	発表学会名	場所	年月日
秋丸裕司、小松(堀井) 美希、岩崎弘登、松田剛典、川本篤彦、澤 芳樹、Piero Anversa、浅原孝之、	ヒトc-kit陽性心筋幹細胞を用いた分化心筋・血管ハイブリッドシートの心筋梗塞モデルへの治療効果	第10回日本再生医療学会	東京	2011/3/1
松浦 勝久 (東京女子医大)	Vascular network formation in cell sheet transplantation and bioengineered three-dimensional tissues	第18回日本血管生物医学会		2010/12/3
Takenori MATSUDA, Daisuke YOSHIOKA, Shigeru MIYAGAWA, Miki KOMATSU, Hiroshi AKIMARU, Atsuhiro SAITO, Atsuhiko KAWAMOTO, Takayuki ASAHARA, Yoshiki SAWA,		75th Japanese Circulation Society	横浜 震災の為 中止	2011/3/20

発表者氏名	発表タイトル	発表学会名	場所	年月日
松田剛典、宮川繁、秋丸裕司、堀井美希、齋藤充弘、川本篤彦、浅原孝之、澤芳樹	心筋再生治療の為のヒト心臓由来C-Kit陽性細胞に対する維持培養法の検討	第10回日本再生医療学会	東京	2011/3/1
増田　治史	Development of in vitro single cell based culture system to assess stem cell fate into endothelial lineage.	第8回ISSCR Annual Meeting	San Francisco	2010/6/16-19

著書

発表者氏名	タイトル	発表誌名	巻号	ページ	出版年
清水　達也	心筋のティッシュエンジニアリング	医学のあゆみ	vol.232 No.5	620-625	2010

IV　研究成果の刊行物・別刷

Published September 20, 2010

Lnk-dependent axis of SCF–cKit signal for osteogenesis in bone fracture healing

Tomoyuki Matsumoto,[1,2] Masaaki Ii,[1,3] Hiromi Nishimura,[1] Taro Shoji,[1,2] Yutaka Mifune,[1,2] Atsuhiko Kawamoto,[1] Ryosuke Kuroda,[2] Tomoaki Fukui,[1,2] Yohei Kawakami,[1,2] Tomoya Kuroda,[1,2] Sang Mo Kwon,[1] Hiroto Iwasaki,[1] Miki Horii,[1] Ayumi Yokoyama,[1] Akira Oyamada,[1] Sang Yang Lee,[2] Shinya Hayashi,[2] Masahiro Kurosaka,[2] Satoshi Takaki,[4] and Takayuki Asahara[1,5]

[1]Group of Vascular Regeneration Research, Institute of Biomedical Research and Innovation, [2]Department of Orthopedic Surgery, Kobe University Graduate School of Medicine, [3]Department of Pharmacology, Osaka Medical College, 565-8686, Osaka, Japan
[4]Division of Immunology, Department of Microbiology and Immunology, Institute of Medical Science, University of Tokyo, Tokyo, 113-0033, Japan
[5]Department of Regenerative Medicine Science, Tokai University School of Medicine, Kanagawa, 251-1193, Japan

The therapeutic potential of hematopoietic stem cells/endothelial progenitor cells (HSCs/EPCs) for fracture healing has been demonstrated with evidence for enhanced vasculogenesis/angiogenesis and osteogenesis at the site of fracture. The adaptor protein Lnk has recently been identified as an essential inhibitor of stem cell factor (SCF)–cKit signaling during stem cell self-renewal, and Lnk-deficient mice demonstrate enhanced hematopoietic reconstitution. In this study, we investigated whether the loss of Lnk signaling enhances the regenerative response during fracture healing. Radiological and histological examination showed accelerated fracture healing and remodeling in Lnk-deficient mice compared with wild-type mice. Molecular, physiological, and morphological approaches showed that vasculogenesis/angiogenesis and osteogenesis were promoted in Lnk-deficient mice by the mobilization and recruitment of HSCs/EPCs via activation of the SCF–cKit signaling pathway in the perifracture zone, which established a favorable environment for bone healing and remodeling. In addition, osteoblasts (OBs) from Lnk-deficient mice had a greater potential for terminal differentiation in response to SCF–cKit signaling in vitro. These findings suggest that inhibition of Lnk may have therapeutic potential by promoting an environment conducive to vasculogenesis/angiogenesis and osteogenesis and by facilitating OB terminal differentiation, leading to enhanced fracture healing.

CORRESPONDENCE
Takayuki Asahara:
asa777@is.icc.u-tokai.ac.jp

Abbreviations used: β-gal, β-galactosidase; AD, adipocyte; ALP, alkaline phosphatase; BMP, bone morphogenetic protein; BMT, BM transplantation; Cbfa1, core binding factor 1; CFU-O, CFU of OB; Col1A1, collagen1A1; EC, endothelial cell; EPC, endothelial progenitor cell; Erk, extracellular signal-related kinase; HSC, hematopoietic stem cell; KSL, cKit$^+$Sca1$^+$Lin$^-$; LDPI, laser Doppler perfusion imaging; micro-CT, micro-computed tomography; MNC, mononuclear cell; OB, osteoblast; OC, osteocalcin; PB, peripheral blood; SCF, stem cell factor; SDS, sodium dodecyl sulfate; SL, Sca1$^+$Lin$^-$; SSC, saline sodium citrate buffer; VCAM, vascular cell adhesion molecule; VE-cad, VE-cadherin.

Embryonic stem cells in the blastocyst stage have the potential to generate any terminally differentiated cells in the body; however, other adult stem cell types, including hematopoietic stem cells/progenitor cells (HSCs/HPCs), have limited potency for postnatal tissue/organ regeneration. The hematopoietic system has traditionally been considered unique among phenotypically characterized adult stem/progenitor cells (Slack, 2000; Blau et al., 2001; Korbling and Estrov, 2003) in that it is an organized, hierarchical system with multipotent, self-renewing stem cells at the top, lineage-committed progenitor cells in the middle, and lineage-restricted precursor cells, which give rise to terminally differentiated cells, at the bottom (Weissman, 2000). Recently, Takaki et al. (2002) reported that Lnk is expressed in hematopoietic cell lineages, and BM cells of Lnk-deficient mice are competitively superior in hematopoietic population to those of WT mice. They also clarified that not only HSC/HPC numbers but also the self-renewal capacity of some HSCs/HPCs were markedly increased in Lnk-deficient mice (Ema et al., 2005). In addition, they identified the functional domains of Lnk and developed a dominant-negative Lnk

The Rockefeller University Press $30.00
J. Exp. Med. Vol. 207 No. 10 2207-2223
www.jem.org/cgi/doi/10.1084/jem.20100321

Published September 20, 2010

mutant that inhibits the functions of Lnk that are endogenously expressed in the HSCs/HPCs and thereby potentiates the HPCs for engraftment (Takizawa et al., 2006). Lnk shares a pleckstrin homology domain, a Src homology 2 domain, and potential tyrosine phosphorylation sites with APS and SH-2B. It belongs to a family of adaptor proteins implicated in integration and regulation of multiple signaling events (Huang et al., 1995; Takaki et al., 1997; Yokouchi et al., 1997; Li et al., 2000; Ahmed and Pillay, 2003) and has also been suggested to act as a negative regulator in the stem cell factor (SCF)–c-Kit signaling pathway (Takaki et al., 2000, 2002).

In another category of regenerative medicine, bone formation and regeneration has been extensively researched to meet clinical demand. A biologically optimal process of fracture repair results in the restoration of normal structure and function in the injured skeletal tissue. Although most fractures heal within a certain time period with callus formation that bridges the fracture gap while bone repair takes place, a large number of patients with fractures lose valuable time because of disability or confinement, leading to a loss of productivity and income. Moreover, a significant amount (5–10%) of fractures fail to heal and result in delayed union or persistent nonunion (Marsh, 1998; Rodriguez-Merchan and Forriol, 2004). Among various causes of failed bone formation and remodeling, inappropriate neoangiogenesis is considered to be a crucial factor (Harper and Kalgsbrun, 1999; Colnot and Helms, 2001). Notably, appropriate vasculogenesis by BM endothelial progenitor cells (EPCs; Asahara et al., 1997) is emerging as a prerequisite for bone development and regeneration, and there appears to be a developmental reciprocity between endothelial cells (ECs) and osteoblasts (OBs; Karsenty and Wagner, 2002). We have recently proved a pathophysiological role and contribution of murine BM-derived $Sca1^+Lin^-$ (SL) cells, HSC/EPC-enriched fraction, for bone healing (Matsumoto et al., 2008). Another group has also reported the increase of $CD34^+/AC133^+$ cells in peripheral blood (PB) of patients with fracture, suggesting the contribution of PB EPCs to bone healing (Laing et al., 2007). However, previous studies have demonstrated that the majority of callus-formed cells in fracture were derived from the periosteum rather than from PB (Nakazawa et al., 2004), indicating a minor contribution of BM-derived cells to fracture healing. Moreover, periosteal cells, but not endosteal BM cells, have recently been shown to be competent to produce fracture callus (Colnot, 2009). Therefore, emerging the concept of enhanced osteogenesis/angiogenesis by HSCs/EPCs, one of the novel factors responsible for stem/progenitor cell mobilization from BM, that is Lnk, attracted our research interests to develop therapeutic strategy using circulating EPCs for bone fracture.

SCF has already been reported to stimulate proliferation and differentiation of HSCs (Broudy, 1997) and mobilize HSCs/EPCs into PB (Mauch et al., 1995; Takahashi et al., 1999) by binding with cKit. Thus, we have investigated the hypothesis that a lack of Lnk signaling, dependent on the SCF–cKit signaling pathway, enhanced the regenerative response via vasculogenesis and osteogenesis in fracture healing by HSC/EPC mobilization and recruitment to sites of fracture in Lnk-deficient mice. In our series of experiments, we showed that a negatively controlled Lnk system contributed to a favorable environment for fracture healing by enhancing vasculogenesis/angiogenesis and osteogenesis via activation of SCF–cKit signaling pathway, which leads to prompt recovery from fracture. In contrast, cKit expression was observed in several tissues and cells, including OBs (Bilbe et al., 1996).

This is the first study showing interaction between the Lnk system and fracture healing that provides a new insight into negatively controlling the Lnk system not only to promote an environment conducive to vasculogenesis/angiogenesis and osteogenesis but also to up-regulate the potential of OB terminal differentiation so that fractures can promptly heal. Therefore, negatively regulating the Lnk system has important implications for the formulation of new therapeutic strategies to enhance bone repair.

RESULTS

Pre- and post-fracture phenotypic characterization of BM and PB

We first attempted to compare the frequency of BM HSC/EPC fraction identified as $cKit^+SL$ (KSL) cells at pre-fracture and 7 d after fracture in Lnk KO mice and age-matched WT mice (C57BL/6). The percentage of BM KSL fraction was significantly higher in post-fracture bone than in pre-fracture bone, regardless of mouse phenotype; however, it was significantly high in both pre- and post-fracture bone in Lnk KO mice compared with WT mice (pre-fracture: Lnk KO, 19.3 ± 0.5, WT, 5.6 ± 0.2; post-fracture: Lnk KO, 23.7 ± 0.5, WT, 8.3 ± 0.4%, respectively; $P < 0.05$ for Lnk KO vs. WT in both pre- and post-fracture bone; pre- vs. post-fracture bone in both Lnk KO and WT; $n = 5$; Fig. 1 a). Also, the number of KSL cells in 10^5 of PB mononuclear cells (MNCs) was significantly greater in post-fracture bone than in pre-fracture bone, regardless of mouse phenotype, and it was significantly great in both pre- and post-fracture PB in Lnk KO mice compared with WT mice (prefracture: Lnk KO, 1,141.4 ± 192.0; WT, 581.9 ± 97.7, post-fracture: Lnk KO, 1,467.1 ± 235.2; WT, 941.9 ± 300.0, respectively; $P < 0.01$ for Lnk KO vs. WT in both pre- and post-fracture; $P < 0.05$ for pre- vs. post-fracture in both Lnk KO and WT; $n = 5$; Fig. 1 b).

We next investigated which cell populations were mobilized into PB under fracture stress. Because the KSL cell population is extremely small in PB, there was no significant difference between the number and the percentage in PB at prefracture and 7 d post-fracture (unpublished data). We therefore attempted to make a comparison of the frequency of PB HSC/EPC-enriched fraction identified as cells at prefracture, 1, 4, 7, and 14 d after fracture in Lnk KO and WT mice. The percentage of post-fracture HSC/EPC-enriched fraction in PB was significantly higher, peaking at day 1 in both Lnk KO and WT mice, than that of pre-fracture (pre-fracture: Lnk KO, 39.7 ± 3.1, WT, 44.9 ± 0.8; 1 d post-fracture: Lnk KO, 56.2 ± 1.6, WT, 59.3 ± 3.1; 4 d post-fracture: Lnk KO, 53.5 ± 3.0, WT, 57.7 ± 1.1; 7 d post-fracture: Lnk KO, 43.8 ± 4.1, WT,

Published September 20, 2010

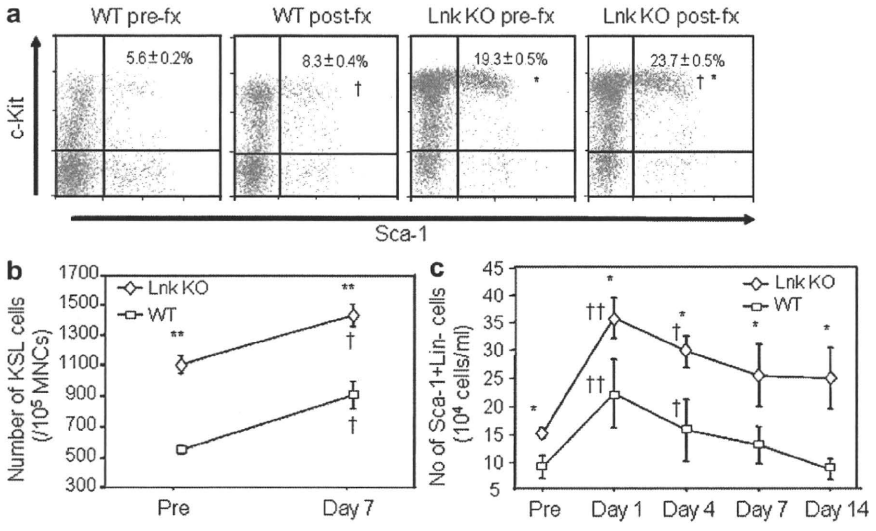

Figure 1. Phenotypic characterization of BM and PB pre- and post-fracture. (a) The percentage of KSL fraction in BMMNCs was assessed by FACS analysis at pre- and 7 d post-fracture (fx) stage in WT and Lnk KO mice, and expressed on the top right quadrant of the dot-blot graph. *, $P < 0.05$ versus WT; †, $P < 0.05$ vs. pre-fx. (b) The number of KSL cells in BMMNCs was also assessed by FACS at pre- and 7 d post-fx stage in WT (open square) and Lnk KO (open rhombus) mice. **, $P < 0.01$ vs. WT; †, $P < 0.05$ vs. pre-fx. (c) The number of SL cells in 1 ml of PB was assessed by FACS in WT (open square) and Lnk KO (open rhombus) mice in the indicated time course. ††, $P < 0.01$; †, $P < 0.05$ versus pre-fx; *, $P < 0.05$ versus WT. All data averaged from five independent experiments. All the mean values with SEM were obtained from triplicated assays.

55.0 ± 1.2; 14 d post-fracture: Lnk KO, 41.0 ± 1.9, WT, 52.6 ± 2.4%; $P < 0.01$ for pre-fracture vs. 1 d post-fracture in both Lnk KO and WT; $P < 0.05$ for pre-fracture vs. 4 d post-fracture in both Lnk KO and WT; $n = 5$). The number of post-fracture SL cells per 1 ml of PB was significantly high, peaking at day 1 compared with pre-fracture (pre-fracture: Lnk KO, 15.1 ± 1.0, WT, 7.2 ± 1.1; 1 d post-fracture: Lnk KO, 35.6 ± 3.7, WT, 22.1 ± 6.1; 4 d post-fracture: Lnk KO, 29.5 ± 2.8, WT, 15.6 ± 9.7; 7 d post-fracture: Lnk KO, 25.3 ± 5.4, WT, 13.7 ± 1.9; 14 d post-fracture: Lnk KO, 24.8 ± 5.4, WT, 8.4 ± 1.9 × 10^4 cells/ml; $P < 0.01$ for pre-fracture vs. 1 d post-fracture in both Lnk KO and WT; $P < 0.05$ for pre-fracture vs. 4 d post-fracture in both Lnk KO and WT, Lnk KO vs. WT at each time point; $n = 5$; Fig. 1 c). These results indicate that both fracture stress and lack of Lnk induce the mobilization of SL cells, including KSL cells from BM, resulting in a high SL/KSL cell number in PB in Lnk KO fractured mice compared with that in WT mice.

Tie2⁺ stem/progenitor cell contribution to vasculogenesis and osteogenesis

Based on the aforementioned evidence, we looked for BM-derived Tie2⁺ stem/progenitor cells in sites of fracture using a mouse BM transplantation (BMT) model. First, we generated Tie2/LacZ Lnk KO mice, in which the LacZ gene is expressed under the regulation of promotor Tie2 (lacking the Lnk gene), by crossing Tie2/LacZ transgenic and Lnk KO mice. We then performed BMT from Tie2/LacZ Lnk KO mice to Lnk KO mice and from Tie2/LacZ WT mice to WT mice. Fracture was induced 4 wk after BMT, after reconstitution of BM with Tie2/LacZ Lnk KO cells in Lnk KO and WT mice, and granulation tissue was analyzed histologically in sites of fracture 7 d after surgery. Double-fluorescent immunostaining was performed for β-galactosidase (β-gal), which can detect BM-derived Tie2⁺ cells and CD31, an EC marker, or for β-gal and osteocalcin (OC). The β-gal⁺ and CD31 double-positive ECs were frequently observed in Tie2/LacZ Lnk KO-BMT Lnk KO mice, whereas the double-positive cells were rarely identified in Tie2/LacZ WT-BMT WT mice (Fig. 2 a). The number of double-positive cells was significantly increased in Tie2/LacZ Lnk KO-BMT Lnk KO mice compared with that in Tie2/LacZ WT-BMT WT mice (Lnk KO, 410.0 ± 37.6 vs. WT, 230.0 ± 56.7/mm²; $P < 0.05$; $n = 3$; Fig. 2 b). The β-gal⁺ and OC double-positive OBs were frequently observed as lining cells along with newly formed bone surface in Tie2/LacZ Lnk KO-BMT Lnk KO mice, whereas only a few double-positive cells were identified in Tie2/LacZ WT-BMT WT mice. (Fig. 2 a) The number of double-positive cells was significantly increased in Tie2/LacZ Lnk KO-BMT Lnk KO mice compared with that in Tie2/LacZ WT-BMT WT mice (Lnk KO, 195.0 ± 31.0 vs.WT, 105.0 ± 21.5/mm²; $P < 0.05$; $n = 3$; Fig. 2 c). These results suggest that enhanced recruitment of mobilized Tie2⁺ stem/progenitor cells to fracture sites contributes to vasculogenesis and osteogenesis, leading to accelerated fracture healing in Lnk KO mice.

BM-derived SL cells exhibit multilineage differentiation potential in vitro

To explore whether SL cells have multilineage differentiation potential, specifically to ECs, OBs, and adipocytes (ADs), BM-derived SL cells were cultured in differentiation induction medium for each lineage, and each marker expression was examined by real-time RT-PCR and immunocytochemistry after culture for 7 and 14 d, respectively. The mRNA expression of EC markers (CD31: 243.8 ± 7.3 vs. 372.1 ± 7.0, $P < 0.05$, $n = 3$; vWF: 49.1 ± 1.0 vs. 396.0 ± 24.1, $P < 0.01$, $n = 3$; Fig. 2 d), OB markers (OC: 6.7 ± 0.8 vs. 182.6 ± 9.5, $P < 0.001$, $n = 3$; Collagen 1-A1: 784.6 ± 107.8 vs. 22,667 ± 2,114, $P < 0.001$, $n = 3$; Fig. 2 e), and AD markers (LPL: 1.4 ± 0.1 vs. 642.0 ± 17.2, $P < 0.0001$, $n = 3$; PPARγ: 7.1 ± 0.3 vs. 162.7 ± 6.7, $P < 0.0001$, $n = 3$; Fig. 2 f) were significantly up-regulated by culture with each lineage induction medium. These lineage marker expressions were further confirmed by

Published September 20, 2010

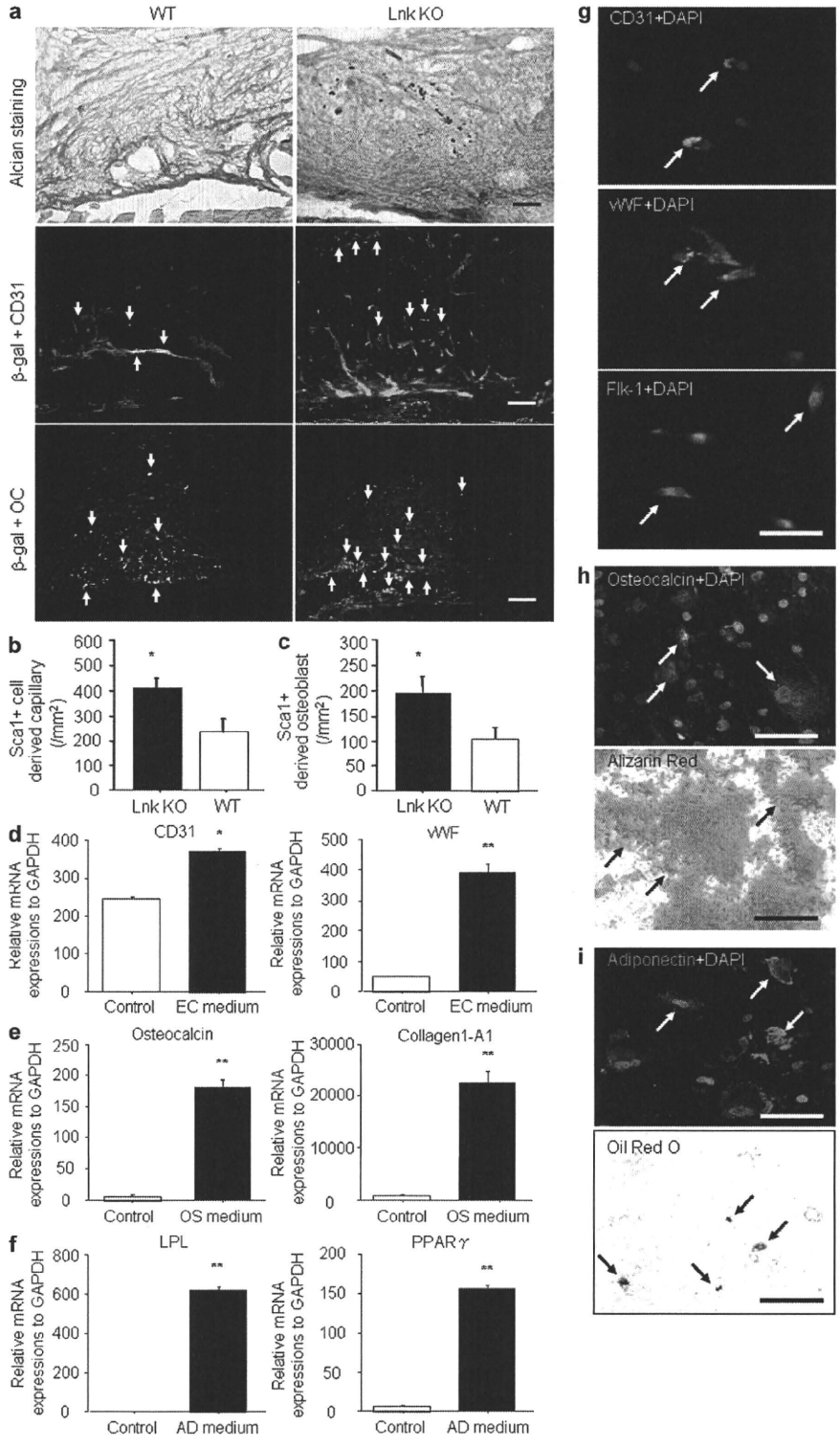

Figure 2. Immunohistochemical detection of Tie2/β-gal⁺ BM-derived stem/progenitor cells in sites of fracture and multilineage differentiation capacity of SL BM cells. (a) Double-immunofluorescent staining for β-gal (red) and CD31 (green) and β-gal (red) and OC (OC, green) were performed in peri-fracture sites 7 d after surgery in Lnk KO mice (left) and WT mice (right). Arrows indicate β-gal/CD31 and β-gal/OC double-positive capillaries and OBs, respectively. Alcian blue/orange G–stained sections were also shown in parallel with immunostained sections. (a, top) Dotted line indicates bone surface. Bars, 50 µm. Quantification of β-gal⁺ ECs (b) and OBs (c). β-gal and CD31 or OC double-positive cells were counted in three randomly selected high-power fields and averaged. *, $P < 0.05$ versus WT. EC (d; CD31 and vWF), OB (e; OC and collagen 1-A1), and AD (f; LPL and PPARγ) marker gene expressions were assessed by real-time RT-PCR in SL cells cultured for 7 d with each cell lineage differentiation medium (*, $P < 0.05$; **, $P < 0.001$) and fluorescent immunostaining analyses with CD31 and vWF for ECs (g), OC for OBs for OBs (h), and LPL and PPARγ for ADs (i) were also performed in SL cells after 14 d in culture. The differentiated SL cells were also stained with alizarin red (h) and oil red O (i) for detecting OB and AD, respectively. Bars, 50 µm. Arrows indicate staining of positive cells. All data averaged with SEM from three independent experiments. All experiments were obtained from triplicated assays.

immunopositivities for CD31, vWF, Flk-1 (Fig. 2 g), OC (Fig. 2 h), and adiponectin (Fig. 2 i) in SL cells. The alizarin red and oil red O staining also show characteristics of OBs and ADs, respectively (Fig. 2, h and i).

Molecular evidence of enhanced angiogenesis and osteogenesis in Lnk KO mice

To explore specific gene expression differences under fracture stress between Lnk-deficient and WT mice, angiogenesis (96)– and osteogenesis (96)–related genes of the tissue at the fracture site spotted on cDNA microarrays were hybridized with biotin-labeled cDNA probes according to the manufacturer's instructions. In angiogenesis gene array, relative expression levels of 12 genes (*ANG*, *Fisp12* [*Ctgf*], *VEGFR*[*Flt1*], *HGF*, *IL-10*, *Gelatinase B* [*Mmp9*], *SR-A* [*Msr1*], *Restin* [*Rsn*], *BM40* [*Sparc*], *ALK-5* [*Tgfbr1*], *THBS1*, and *VCAM-1*) of Lnk-deficient fractured mice increased by >1.5-fold, but 5 genes (*Ephrin B4* [*Ephb4*], *IFNr* [*Ifng*], *NOS3*, *Osteopontin* [*Spp1*], and *THBS2*) decreased by >2-fold compared with WT fractured mice (Fig. 3 a). In osteogenesis gene array, 24 genes (*annexin A5* [*Anxa5*], *OC* [*Bglap1*], *Bgn*,

Published September 20, 2010

Alk-6 [*Bmpr1a*], *BMPR2*, *Col11a1*, *Col1a1*, *Col1A2*, *Col4a6*, *Col6a2*, *Ctsk*, *Dcn*, *FLG* [*Fgfr1*], *Smad2* [*Madh1*], *Smad3* [*Madh3*], *Collagenase-3* [*Mmp13*], *MMP8*, *Gelatinase B* [*Mmp9*], *Osf2/Cbfa1* [*Runx2*], *SPARC*, *TGFb3*, *ALK-5* [*Tgfbr1*], *VCAM-1*, and *Vdr*) of Lnk-deficient fractured mice increased by >1.5-fold compared with WT fractured mice ($n = 3$; Fig. 3 b).

Real time RT-PCR analysis of the tissue that was RNA isolated from the peri-fracture site was also performed in the expression of several key genes as a quantitative analysis. The results demonstrated a significantly higher expression of EC markers (CD31, VE-cadherin [VE-cad], and KDR/Flk1) in Lnk KO group compared with WT group (CD31: Lnk KO, 5.803 ± 0.667, WT, 1.171 ± 0.029, $P < 0.01$; VE-cad: Lnk KO, 7.693 ± 0.602, WT, 1.244 ± 0.006, $P < 0.01$; KDR: Lnk KO, 11.082 ± 1.036, WT, 1.415 ± 0.035, respectively, $P < 0.01$; $n = 3$; Fig. 3 c). The expression of bone-related

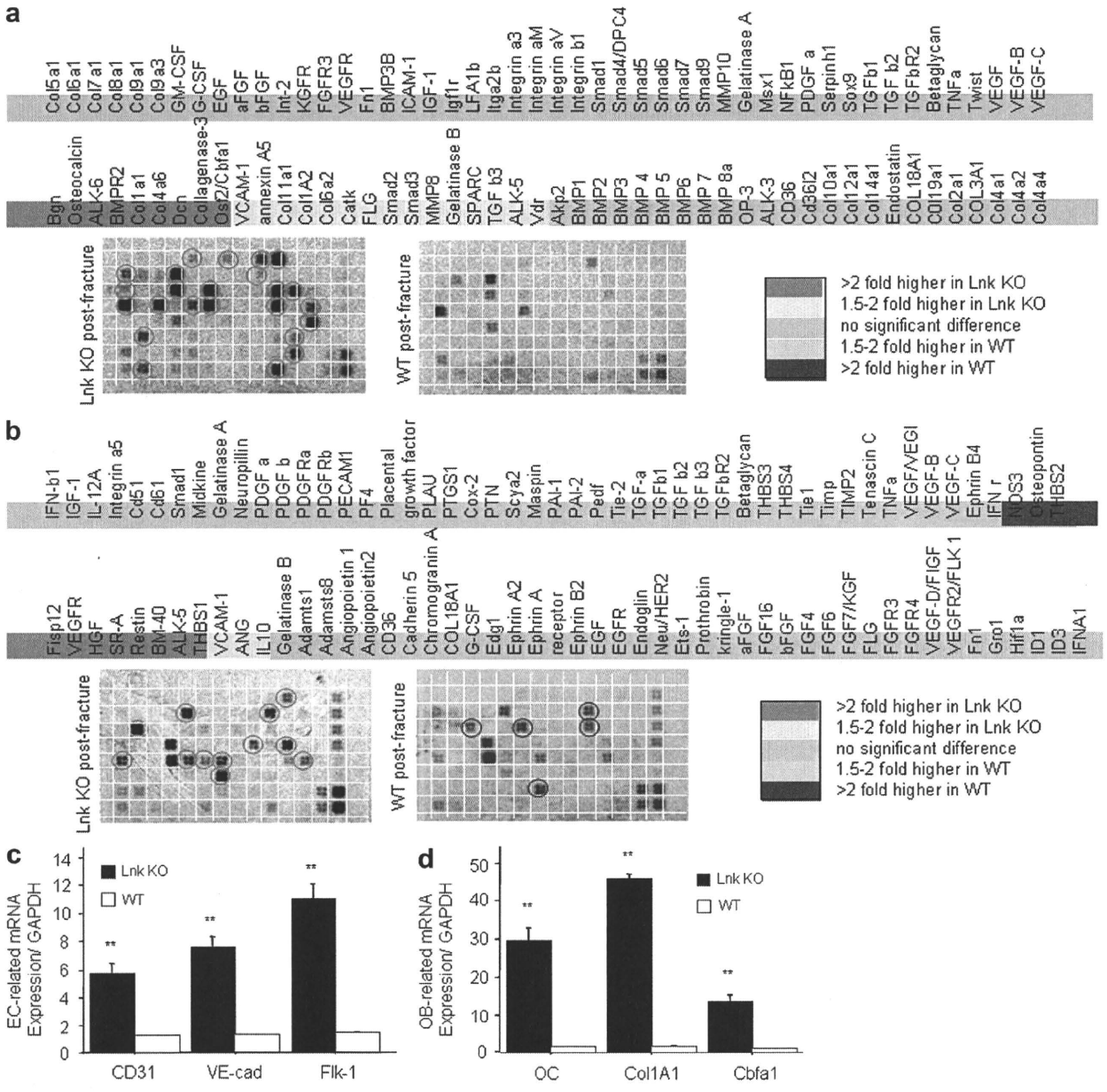

Figure 3. Angiogenesis- and osteogenesis-related gene expressions in sites of fracture. (a and b) A series of gene expressions detected by DNA microarray analysis in granulation tissue samples of peri-fracture sites 7 d after surgery in Lnk KO and WT mice. Red circles indicate >1.5-fold and blue circles do over 2-fold-increased blots in Lnk KO mice compared with WT mice. The selected EC-related (c) and OB-related (d) gene up-regulation in the same samples as those in DNA microarray analysis were further confirmed by quantitative real-time RT-PCR analysis. VE-cad, Flk-1 (VEGF receptor 2); Col1A1, Col1A1; and Cbfa1, Cbfa1. **, $P < 0.01$ versus WT. All data averaged with SEM from three independent experiments. All experiments were obtained from triplicated assays.

Published September 20, 2010

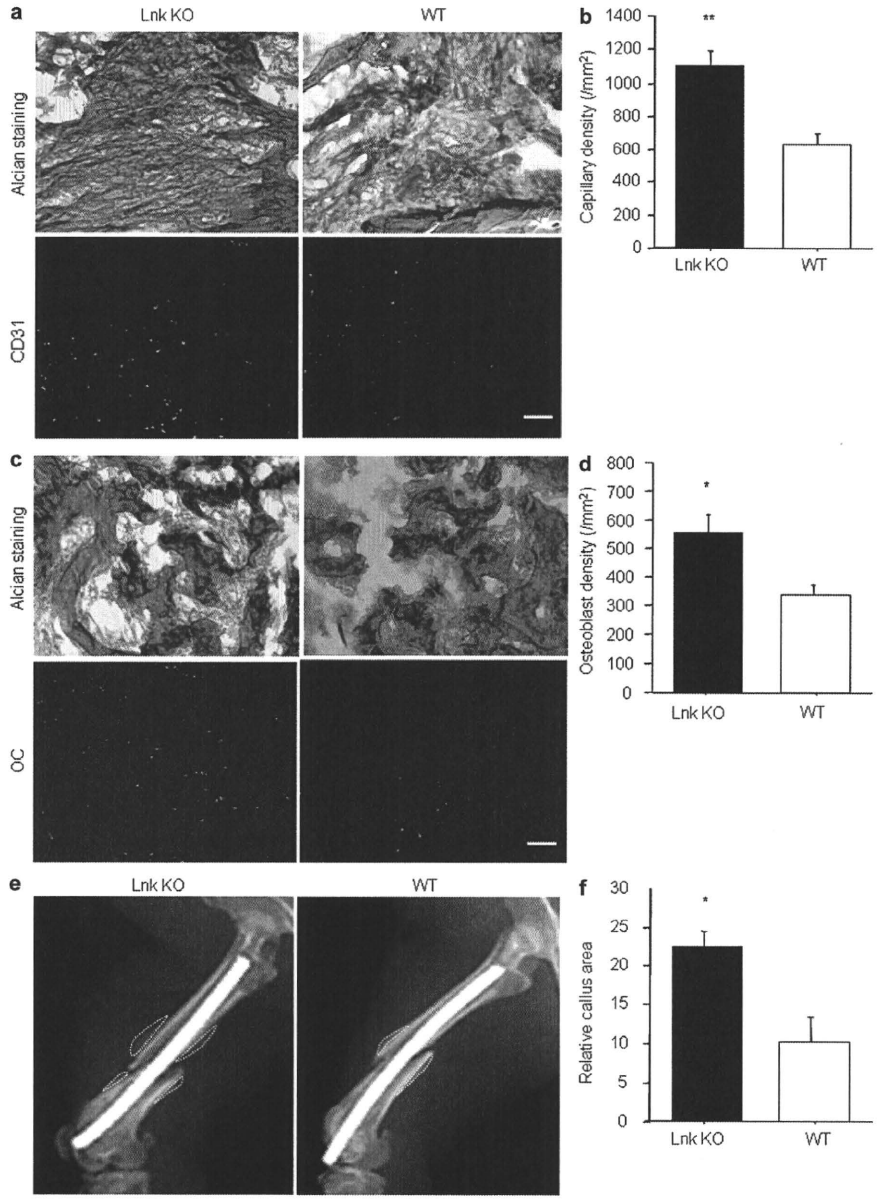

Figure 4. Histological and radiographical evidences of enhanced angiogenesis/vasculogenesis and osteogenesis in Lnk KO fractured mice. Immunofluorescent staining for CD31 (green; a) and OC (OC, green; c) were performed in granulation tissue samples of peri-fracture sites in Lnk KO (left) and WT (right) mice 7 d after fracture. Alcian blue/orange G-stained sections were also shown in parallel with immunostained sections. (bottom) Dotted line indicates bone surface. Bar, 50 µm. Quantification of capillaries (b) and OBs (d). CD31 positive capillaries and OC positive OBs were counted in 3 randomly selected high power fields and averaged. **, $P < 0.01$ versus WT. (e) Radiographical assessment of callus area in sites of fracture 7 d after surgery. Callus area is indicated in dotted line. (f) Relative callus areas are quantified and averaged. *, $P < 0.05$ versus WT. All data averaged with SEM from three independent experiments. All experiments were obtained from triplicated assays.

markers (OC, collagen1A1 [Col1A1], and Core binding factor 1 [Cbfa1]) were significantly enhanced in Lnk KO group compared with WT group (OC: Lnk KO, 29.707 ± 3.116, WT, 1.294 ± 0.056, $P < 0.01$; Col1A1: Lnk KO, 46.189 ± 0.870, WT, 1.225 ± 0.225, $P < 0.01$; Cbfa1: Lnk KO, 13.586 ± 1.767; WT, 0.999 ± 0.049, $P < 0.01$; $n = 3$; Fig. 3 d). These results indicate the enhancement of osteogenesis, as well as angiogenesis, at fracture sites in Lnk KO mice.

Morphological evidence of enhanced angiogenesis and osteogenesis in fractured Lnk KO mice

Enhanced angiogenesis and osteogenesis were further confirmed by immunohistochemistry. Vascular staining with CD31 (marker for mouse EC) 7 d after fracture demonstrated enhanced neovascularization around the endochondral ossification area in Lnk KO mice compared with that in WT mice (Fig. 4 a). Neovascularization assessed by capillary density was significantly enhanced in Lnk KO mice compared with that in WT mice (Lnk KO, 1,101.8 ± 97.7 vs. WT, 628.7 ± 28.5/mm²; $P < 0.01$; $n = 3$; Fig. 4 b).

OB staining with OC (marker for mouse OB) 7 d after fracture also revealed the augmentation of osteogenesis in newly formed bone area in Lnk KO mice compared with WT mice (Fig. 4 c). Osteogenesis assessed by OB density was significantly enhanced in Lnk KO mice compared with WT mice (Lnk KO, 111.7 ± 13.2, WT, 66.7 ± 6.5/mm²; $P < 0.05$; $n = 3$; Fig. 4 d). Callus formation was monitored radiographically to evaluate fracture healing process, and the relative callus areas detected by radiography were quantified at week 1 in Lnk KO and WT group (Fig. 4 e). The relative callus area was significant larger in the Lnk KO group compared with the WT group (Lnk KO, 22.3 ± 2.0, WT, 10.0 ± 3.0; $P < 0.05$; $n = 3$; Fig. 4 f). These results indicate the morphological enhancement of angiogenesis and osteogenesis in Lnk KO mice compared with WT mice in fracture-induced environment.

Physiological, radiological, and histological evidences of promoted fracture healing in Lnk KO mice

Blood perfusion and morphological fracture healing in each group was evaluated by laser Doppler perfusion imaging (LDPI)

Published September 20, 2010

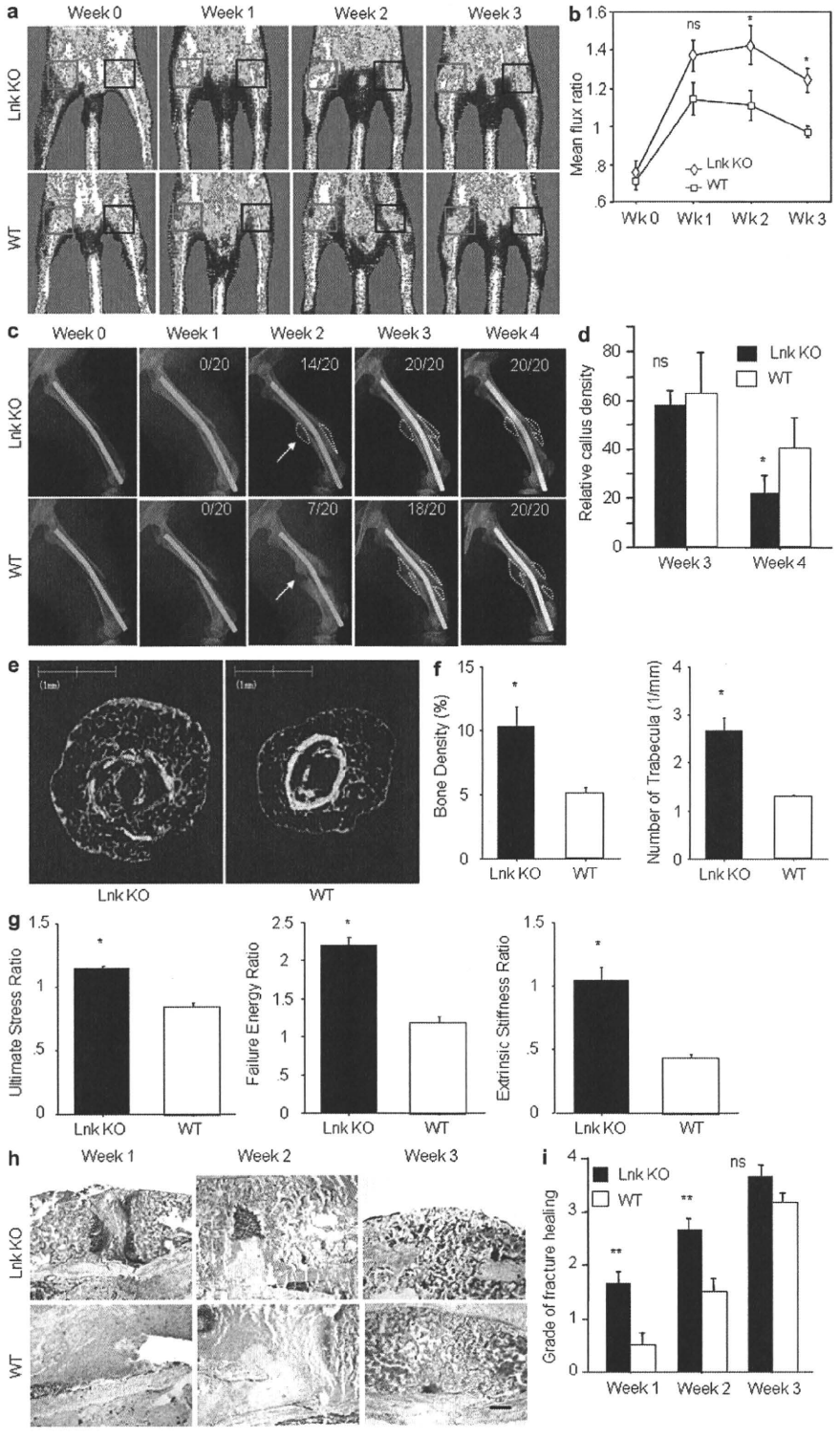

Figure 5. Increased blood perfusion and radiographically accelerated fracture healing in Lnk KO mice. (a) Tissue blood perfusion evaluated by LDPI system after surgery in the indicated time course. The fractured sites are indicated in red square and intact contra-lateral sites are indicated in black square. (b) The mean flux-ratio was calculated by dividing mean flux value in red square with that in blue square and expressed as a relative mean flux value. **, $P < 0.01$ versus Week 0 and *, $P < 0.05$ versus WT. Data averaged with SEM from four independent experiments. Radiographical (c and e) and histological (f) assessment during fracture healing process in Lnk KO (left) and WT (right) mice. (c) Callus area is indicated in dotted line and the number of healed bones out of 20 is indicated in upper right corner of the image. Arrows indicate fracture sites. (d) The number of relative callus density is quantified. * and ns, $P < 0.05$ versus WT, $n = 20$ each. (e) The bone structure after healing was further assessed by micro CT 28 d after surgery. (f) Bone density and number of trabecular bones were quantified in the micro CT images and averaged. *, $P < 0.05$ versus WT. Data averaged with SEM from four independent experiments. (g) Biomechanical function test for healed bone in Lnk KO and WT mice 28 d after fracture. Each parameter, ultimate stress (left), fracture energy (center) and extrinsic stiffness ratio (right), was evaluated as healed bone function. *, $P < 0.05$ versus WT. Data averaged with SEM from four independent experiments. (h) Toluidine blue staining was performed with granulation tissue at fracture site in the indicated time course. Chondrocytes are stained in blue and bone including newly formed trabecular bone is appeared in gray. Bar = 200 µm. (i) The degree of fracture healing in the toluidine blue stained sections was assessed by Allen's classification in Lnk KO and WT mice. ** and ns, $P < 0.01$ versus WT. Data averaged with SEM from six independent experiments.

system and radiological examinations at subsequent time points after fracture. LDPI analysis (Fig. 5 a) demonstrated a severe loss of blood flow at the fracture sites 1 h after fracture creation in both groups. However, the blood flow of the fractured limb increased until 2 wk post-fracture, and then decreased slowly in KO mice. In WT mice, the blood flow showed a mild increase until 1 wk post-fracture, and then decreased. In both groups, the ratio of fractured/intact (contralateral) blood flow significantly increased by week 1 (Fig. 5 b). There was no significant difference in the ratio 1 h after fracture creation between the groups, whereas the ratio at weeks 1, 2, and 3 were significantly higher in Lnk KO mice compared with WT mice (0 wk: Lnk KO, 0.753 ± 0.067, WT,

Published September 20, 2010

0.707 ± 0.045; 1 wk: Lnk KO, 1.370 ± 0.081, WT, 1.144 ± 0.088; 2 wk: Lnk KO, 1.425 ± 0.103, WT, 1.110 ± 0.077; 3 wk: Lnk KO, 1.241 ± 0.064, WT, 0.972 ± 0.030; $P < 0.01$ for week 0 vs. weeks 1–3 in both Lnk KO and WT; $P < 0.05$ for Lnk KO vs. WT in week 1–3; $n = 4$ mice/group/time-point; Fig. 5 b).

In 70% (14 out of 20) of Lnk KO mice at week 2 and 100% (20 out of 20) at week 3, the fracture healed with bridging callus formation radiographically, whereas in WT mice only 35% (7 out of 20) had healed at week 2 and 90% (18 out of 20) at week 3 ($P < 0.05$ in week 2; Fig. 5 c), which is consistent with the data in previous studies demonstrating the natural course in this animal model (Manigrasso and O'Connor, 2004). To evaluate bone remodeling, bone absorption was monitored radiographically and relative callus density was quantified at week 3 and 4 in Lnk KO and WT group. Relative callus density was significantly lower in Lnk KO group compared with that in WT group (3 wk: Lnk KO, 58.1 ± 2.4 vs. WT, 62.2 ± 6.8, ns; 4 wk: Lnk KO, 22.5 ± 2.8 vs. WT, 40.2 ± 5.3, $P < 0.05$, $n = 20$; Fig. 5 d).

Morphological and functional fracture healing in each group was further evaluated by micro-computed tomography (micro-CT), histological analysis, and biomechanical examination 28 d after fracture surgery. The micro-CT results showed striking trabecular bone formation in Lnk KO mice compared to that in WT mice (Fig. 5 e). Quantitative analysis for bone formation was performed with micro-CT images and expressed as bone density (Fig. 5 f, left) and trabecula number (Fig. 5 f, right). Both parameters were significantly high in Lnk KO mice compared with that in WT mice (bone density: Lnk KO, 10.4 ± 1.5 vs. WT, 5.0 ± 0.3, $P < 0.05$, $n = 4$; number of trabecular: Lnk KO, 2.7 ± 0.3 vs. WT, 1.3 ± 0.03, $P < 0.01$, $n = 4$; Fig. 5 f). Biomechanical examinations by three-point bending test also showed significantly increased ultimate stress ratio (Lnk KO, 1.2 ± 0.02 vs. WT, 0.8 ± 0.03, $P < 0.001$, $n = 4$), failure energy ratio (Lnk KO, 2.2 ± 0.1 vs. WT, 1.2 ± 0.1, $P < 0.001$, $n = 4$), and extrinsic stiffness ratio (Lnk KO, 1.1 ± 0.1 vs. 0.4 ± 0.04, $P < 0.01$, $n = 4$; Fig. 5 g).

Histological evaluation with toluidine blue staining demonstrated the enhanced endochondral ossification consisting of numerous chondrocytes and newly formed trabecular bone at week 1, bridging callus formation at week 2, and complete union at week 3 in Lnk KO mice. In contrast, although a callus formation was observed at week 1, bridging callus formation was rarely found at week 2 in WT mice (Fig. 5 h). The degree of fracture healing assessed by Allen's classification (Allen et al., 1980) was significantly higher in the Lnk KO group compared with the WT group at week 1 and 2 (1 wk: Lnk KO, 1.67 ± 0.21 vs. WT, 0.50 ± 0.22; 2 wk: Lnk KO, 2.67 ± 0.21 vs. WT, 1.50 ± 0.22, $P < 0.01$, $n = 6$; 3 wk: Lnk KO, 3.67 ± 0.21 vs. WT, 3.17 ± 0.17, ns, $n = 6$; Fig. 5 i). These results indicate that Lnk KO mice have a potential for prompt fracture healing evaluated by not only radiographical analysis but also biomechanical functional examination.

Critical role of SCF–cKit signaling in enhanced SL cell mobilization from BM and recruitment to sites of fracture

Although the aforementioned results clearly demonstrated enhanced vasculogenesis/angiogenesis and osteogenesis via SL or $Tie2^+$ cell mobilization into PB and recruitment to sites of fracture in Lnk KO mice, the precise mechanism remains unclear. To explore the possible mechanism, we focused on the role of the stem/progenitor cell chemokine SCF, which is a ligand for the receptor cKit, in Lnk KO mice as well as in WT mice. Accordingly, mouse (m) SCF plasma levels were measured before and after fracture at subsequent time points in both types of mice. The plasma SCF levels were decreased after fracture surgery regardless of Lnk gene deficiency in mice; however, the extent of decrease was significantly limited during the fracture healing process and returned to over the baseline level at day 14 in Lnk KO mice compared with that in WT mice (prefracture: Lnk KO, 263.4 ± 9.4 vs. WT, 251.0 ± 35.6 pg/ml; ns and 1 d post-fracture: Lnk KO, 194.1 ± 11.7 vs. WT, 166.8 ± 12.7 pg/ml; 4 d post-fracture: Lnk KO, 197.7 ± 7.2 vs. WT, 181.5 ± 28.9 pg/ml; 7 d post-fracture: Lnk KO, 214.7 ± 20.6 vs. WT, 190.7 ± 24.0 pg/ml; and 14 d post-fracture: Lnk KO, 284.2 ± 19.7 vs. WT, 207.3 ± 16.6 pg/ml; $P < 0.01$ for each comparison; $n = 5$; Fig. 6 a).

Next, the gain and loss of function test of SCF for SL cell mobilization in PB was performed by FACS analysis. We intraperitoneally injected 20 μg/kg mSCF, soluble SCF receptor (sKit, antagonist of SCF; Turner et al., 1995; Nakamura et al., 2004), or PBS into unfractured Lnk KO or WT mice for 5 d and examined SL cell kinetics in PB. The number of SL cells significantly increased, peaking at day 7 after SCF stimulation in Lnk KO mice, but not in WT mice, and no SL cell number increase was observed in the other treatment groups (sKit treatment in Lnk KO mice and PBS treatment in Lnk KO mice and in WT mice; prestimulation: Lnk KO-PBS, 13.0 ± 1.3; Lnk KO-SCF, 13.1 ± 0.7; Lnk KO-sKit, 15.3 ± 0.2; WT-PBS, 8.1 ± 0.9; WT-SCF, 8.7 ± 0.6 × 10^4 cells/ml, ns, $n = 5$; 7 d post-stimulation: Lnk KO-SCF, 73.4 ± 4.1 vs. Lnk KO-PBS, 15.3 ± 2.5; Lnk KO-sKit, 10.0 ± 0.8; WT-PBS, 8.3 ± 0.3; and WT-SCF, 12.8 ± 2.4 × 10^4 cells/ml, $P < 0.05$, $n = 5$; and 14 d post-fracture: Lnk KO-SCF, 39.2 ± 6.2 vs. Lnk KO-PBS, 13.6 ± 9.7; Lnk KO-sKit, 12.0 ± 0.3; WT-PBS, 7.9 ± 0.9; and WT-SCF, 10.0 ± 0.9 × 10^4 cells/ml, $P < 0.01$, $n = 5$; Fig. 6 b). Next, to identify the synergistic effect of fracture stress and SCF stimulation on SL cell mobilization, SCF with or without sKit and PBS was injected into fractured WT mice, and sKit alone was injected into fractured Lnk KO mice in the same way. In the fractured WT mice, the number of SL cells was significantly increased, peaking at day 7 post-stimulation by SCF, but not by PBS, whereas no response of SL cell number was observed in nonfractured WT mice by SCF, and the effect of SCF on SL cell mobilization was completely cancelled by coinjection of sKit. The inhibitory effect of sKit on SL cell mobilization in PB was also observed partially in Lnk KO mice with fracture (prestimulation: Lnk KO-sKit-Fx, 16.7 ± 2.1 vs. WT-PBS-Fx, 9.0 ± 2.1; WT-SCF-Fx, 8.3 ± 0.7; and WT-SCF-sKit-Fx, 9.8 ± 0.7 × 10^4 cells/ml, $P < 0.05$,